Differential nickel-induced responses of olfactory sensory neuron populations in zebrafish

Maurizio Lazzari[*,1], Simone Bettini[1], Liliana Milani, Maria Gabriella Maurizii, Valeria Franceschini

Department of Biological, Geological and Environmental Sciences, University of Bologna, 40126 Bologna, Italy

A B S T R A C T

The olfactory epithelium of fish includes three main types of olfactory sensory neurons (OSNs). Whereas ciliated (cOSNs) and microvillous olfactory sensory neurons (mOSNs) are common to all vertebrates, a third, smaller group, the crypt cells, is exclusive for fish. Dissolved pollutants reach OSNs, thus resulting in impairment of the olfactory function with possible neurobehavioral damages, and nickel represents a diffuse olfactory toxicant. We studied the effects of three sublethal Ni^{2+} concentrations on the different OSN populations of zebrafish that is a widely used biological model. We applied image analysis with cell count and quantification of histochemically-detected markers of the different types of OSNs. The present study shows clear evidence of a differential responses of OSN populations to treatments. Densitometric values for $G_{\alpha\ olf}$, a marker of cOSNs, decreased compared to control and showed a concentration-dependent effect in the ventral half of the olfactory rosette. The densitometric analysis of TRPC2, a marker of mOSNs, revealed a statistically significant reduction compared to control, smaller than the decrease for $G_{\alpha\ olf}$ and without concentration-dependent effects. After exposure, olfactory epithelium stained with anti-calretinin, a marker of c- and mOSNs, revealed a decrease in thickness while the sensory area appeared unchanged. The thickness reduction together with increased densitometric values for HuC/D, a marker of mature and immature neurons, suggests that the decrements in $G_{\alpha\ olf}$ and TRPC2 immunostaining may depend on cell death. However, reductions in the number of apical processes and of antigen expression could be a further explanation. We hypothesize that cOSNs are more sensitive than mOSNs to Ni^{2+} exposure. Difference between subpopulations of OSNs or differences in water flux throughout the olfactory cavity could account for the greater susceptibility of the OSNs located in the ventral half of the olfactory rosette. Cell count of anti-TrkA immunopositive cells reveals that Ni^{2+} exposure does not affect crypt cells. The results of this immunohistochemical study are not in line with those obtained by electro-olfactogram.

1. Introduction

The olfactory organ of fish is in direct contact with the environmental water, therefore dissolved chemical pollutants can directly affect neurological functions of olfactory sensory neurons (OSNs)(Laberge and Hara, 2001; Sorensen and Caprio, 1998; Tierney et al., 2010; Zielinski and Hara, 2006).

Different types of fish OSNs can be distinguished by morphological characteristics and their response to particular odors (Hansen et al., 2003; Zielinski and Hara, 2006). Vertebrates possess two main types of OSNs, ciliated (cOSNs) and microvillous olfactory sensory neurons (mOSNs) (Eisthen, 1992; Zielinski and Hara, 2006). In fish belonging to elasmobranchs, cladistians and teleosts an additional group of OSNs

was described, the crypt cells (Ferrando et al., 2006, 2007, 2011; Hansen and Finger, 2000). Bundles of OSN axons constitute the olfactory nerve that enters the olfactory bulb of the telencephalon in which they form synaptic contacts with dendrites of mitral cells and local interneurons in the glomerular layer (Hamdani and Døving, 2007).

OSNs show different olfactory signaling pathways. cOSNs and crypt cells have a cAMP-mediated olfactory signaling pathway, whereas mOSNs possess an IP3-based pathway. The response of specific classes of OSNs to specific odors can be determined by exploiting differences in these pathways (Hansen et al., 2003; Kolmakov et al., 2009; Laframboise and Zielinski, 2011; Michel et al., 2003; Rolen et al., 2003). For example, a histological technique has demonstrated the specific action of taurocholic acid on cOSNs (Bazáes and

---

Schmachtenberg, 2012; Døving et al., 2011; Vielma et al., 2008). Moreover, changes in the response of OSNs to specific odors can be used to determine how a certain contaminant affects a specific type of OSNs (Dew et al., 2014, 2016).

Freshwater ecosystems are heavily affected by discharge of domestic, industrial and agricultural wastewaters (Katagi, 2010; Klečka et al., 2010; Schwarzenbach et al., 2010). Therefore, an efficient monitoring should identify quickly environmental modifications that require a rapid reaction. Fish have been recognized as particularly suited organisms for environmental biomonitoring due to some of their characteristics, including biodiversity, health conditions and population structure (Chua et al., 2018). Fish have also become a system of choice for in vivo and in vitro toxicity tests (Cardwell et al., 1976; Kollár et al., 2018). Normal embryo conditions, including embryo growth, egg hatchability, survival, gene expression and DNA damage represent other monitoring criteria in fish (Boran and Şaffak, 2018; Lammer et al., 2009a, b). Many metals are neurotoxic chemicals present as contaminants in the aquatic environment and they can affect chemosensory functions, causing "info-disruption" (Lürling and Scheffer, 2007) and severe decline in olfaction in vertebrates (Baldwin et al., 2011; Bondier et al., 2008, Hentig and Byrd-Jacobs, 2016). In fish, some metals can cause severe neurobehavioral damages ranging from slight alterations to loss of olfactory-controlled behaviors that are basic to survival (Baldwin et al., 2003; Dew et al., 2014, 2016; Hentig and Byrd-Jacobs, 2016; Sandahl et al., 2007; Scott et al., 2003).

Human activities, including agriculture, urban life and industry, have been identified as the main sources of nickel found in waters (Tiller, 1989). Increased levels of nickel in waters can be harmful to animals, humans included (Alam et al., 2008; White et al., 2016). As a diffusible contaminant, nickel is found in urban runoff at a low concentration (2–37 µg/L; Soller et al., 2005). Nickel is a diffusible neurotoxic agent exerting its effect on fish olfaction (Dew et al., 2014; Giattina et al., 1982; Lari et al., 2018; Tierney et al., 2010). The mechanisms by which nickel affects olfaction are still under investigation (Calderón-Garcidueñas, 2015; Dew et al., 2014, 2016; Tierney, 2016; Topal et al., 2015).

This work is aimed at studying the histopathological reactions in the three different types of OSNs, ciliated, microvillous and crypt neurons, in zebrafish exposed to sub-lethal concentrations of nickel ions (Ni^{2+}). Neuronal responses to Ni^{2+} exposure were evaluated by means of image analysis quantification of neuronal markers detected by immunohistochemical staining. Possible resultant electrophysiological or behavioral changes will deserve subsequent extensive investigation.

The current literature includes data about toxicity in different species, of different metals and under different experimental conditions; this multiplicity of experimental set-ups makes a comparisons quite difficult (Azizishirazi et al., 2013; Song et al., 2015; Tierney et al., 2010; Wang et al., 2013a). The present research was conducted on the freshwater fish *Danio rerio*, zebrafish, which is worldwide used for genetic, embryological and neurological studies. The use of zebrafish in toxicity evaluation relies on its significant advantages as a model organism, including reduced housing costs and small size of specimens that permits quantitative analysis on a reduced number of tissue slices (Hill et al., 2005; Miyasaka et al., 2013; Segner, 2009). The choice of zebrafish also depends on its broad use in the study of the olfactory system, histologically comparable to that of other vertebrates (Tierney et al., 2010), and the possibility to clearly characterize the cells constituting its olfactory neuroepithelium by immunological approaches (Braubach et al., 2012; Gayoso et al., 2011; Germanà et al., 2007).

2. Materials and methods

2.1. Animals

The study was carried out on 40 adult zebrafish (*Danio rerio*, Hamilton, 1882) including males and females, 6–8 months old and 4 cm total length, purchased from the Coral Aquarium, Bologna, Italy. Acclimatization took place in tanks containing dechlorinated tap water and distilled water (1:2) for one month, at 25 °C in a 12:12 h light-dark cycle. They were fed twice a day by an automatic fish feeder. All procedures followed the guidelines of European Community Council Directive (86/609/CEE), the current Italian legislation on the use and care of animals, and the guidelines issued by the US National Institutes of Health. Ethical approval of this study was obtained from the Scientific Ethics Committee of the University of Bologna (protocol no. 17/79/2014).

2.2. Nickel exposure

In the US EPA ECOTOX database (http://cfpub.epa.gov/ecotox/), the LC_{50} for nickel chloride measured in adults and juveniles exposed for 48 h was > 10 mg L^{-1}. In the present study, three nickel ion concentrations, supposed to be sub-lethal, were prepared from nickel chloride hexahydrate (Merck, Darmstadt, Germany) dissolved in acclimatization water: low quantity (LQ), 0.4 mg L^{-1} of nickel chloride hexahydrate, corresponding to 0.1 mg L^{-1} of Ni^{2+}; medium quantity (MQ), 2 mg L^{-1} of nickel chloride hexahydrate, corresponding to 0.5 mg L^{-1} of Ni^{2+}; high quantity (HQ), 4 mg L^{-1} of nickel chloride hexahydrate, corresponding to 1 mg L^{-1} of Ni^{2+}. The concentrations of 0.5 mg L^{-1} correspond to the environmentally relevant nickel level used by Macomber et al. (2011); 0.1 mg L^{-1} and 1 mg L^{-1} are five times lower and two times greater, respectively. These values partially correspond to Ni^{2+} concentrations used by Dew et al. (2014) in their electrophysiological and behavioral study (0.05, 0.1, and 0.5 mg L^{-1} of Ni^{2+}). These authors drew attention to environmental relevance of these Ni^{2+} concentrations since these values are able to alter olfaction of fish and consequently their behavior in the environment. The Ni^{2+} concentration of 1 mg L^{-1}, still lower than LC_{50} (> 10 mg L^{-1} Ni^{2+}; US EPA ECOTOX database, http://cfpub.epa.gov/ecotox/), can be found in case of extensive but still sub-lethal nickel pollution. In the wild, the concentrations of such ions can range in a wide interval, although usually at lower scale than the concentrations we used in this study. The choice we did was based on LC50 values and on what was reported in Dew et al. (2014), thus to consider concentrations at which an ob-servable damage was likely produced, although keeping the parameter at a sublethal level. Ten fish were transferred into each of three 10 L tanks containing 0.1, 0.5, and 1 mg L^{-1} of Ni^{2+}. Employing a static/renewal system, fish were transferred to new tanks containing freshly prepared Ni^{2+} solutions every 24 h. The olfactory toxicity of the 3 nickel ion concentrations was evaluated in fish sacrificed after standard 4-day (96 h) exposure, according to common use in acute toxicity tests. Ten control fish were maintained in acclimatization water, changed every 24 h. Control animals were sacrificed at the same time as treated fish. The water parameters of acclimatization, treatment, and control tanks were monitored. Their representative values are reported in Table 1.

2.3. Tissue

Fish were anesthetized with 0.1% 3-aminobenzoic acid ethyl ester (MS-222, Sigma, St. Louis MO, USA) dissolved in Ni^{2+} containing water (treated specimens) or acclimatization water (controls) and killed by decapitation. The dorsal cranium was quickly removed, and then the heads were immersion-fixed in a modified Bouin's fixative solution composed of saturated aqueous solution of picric acid and formalin, ratio 3:1, for 24 h at room temperature.

After fixation, picric acid was removed by long washing in fre-quently renewed 0.1 M phosphate buffer. The heads were decalcified in 0.25 M EDTA in 0.1 M phosphate buffer, pH 7.4, for 9 days at room temperature, dehydrated and then embedded in Paraplast Plus (Leica Biosystems, Richmond, IL, USA; melting point 55–57 °C). Five µm-thick serial frontal sections were collected on silane-coated slides (Sigma).

Table 1
Water parameters of acclimation, control, and Ni^{2+} exposure tanks.

	NO$_3$ mg L^{-1}	NO$_2$ mg L^{-1}	GH dH	KH dH	pH
Acclimatization tanks, new water, before fish insertion	< 25	< 0.5	14–21°	10	7.4–7.5
Acclimatization tanks, after 24 h fish presence, before water change	< 25	< 0.5	14–21°	10	7.3–7.4
Control tanks, new water, before fish insertion	< 25	< 0.5	14–21°	10	7.4–7.5
Control tanks, after 24 h fish presence, before water change	< 25	< 0.5	14–21°	10	7.3–7.4
Exposure tanks, new water, before fish insertion	< 25	< 0.5	14–21°	10	7.4–7.5
Exposure tanks, after 24 h fish presence, before water change	< 25	< 0.5	14–21°	10	7.3–7.4

dH, degree of hardness; GH, general hardness; KH, carbonate hardness.

Adjacent slides were used for immunohistochemical detection.

2.4. Immunohistochemistry

Detailed method is reported in Lazzari et al. (2016). After deparaffinization and rehydration, sections were incubated separately with five primary antibodies, in a moist chamber on a floating plate at 4 °C overnight: a) rabbit polyclonal anti-calretinin (AB5054; Chemicon International, Temecula, CA, USA; used dilution 1:1,000) that in zebrafish detects a heterogeneous population of ciliated and microvillous olfactory neurons (Bettini et al., 2016); b) rabbit polyclonal anti-G$_{\alpha}$ olf (sc-385; Santa Cruz Biotechnology, Santa Cruz, CA, USA; used dilution 1:500), a marker for ciliated olfactory neurons (Braubach et al., 2012; Gayoso et al., 2011); c) rabbit polyclonal anti-transient receptor potential cation channel, subfamily C, member 2 (anti-TRPC2; LS-C95010; LifeSpan BioSciences, Seattle, WA, USA; used dilution 1:200), a marker for microvillous olfactory neurons (Bettini et al., 2016); d) rabbit polyclonal anti-tyrosine protein kinase A (anti-TrkA; sc-118; Santa Cruz Biotechnology; used dilution 1:100), a marker for crypt olfactory cells in zebrafish (Ahuja et al., 2013; Bettini et al. 2016); e) mouse mono-clonal anti-human neuronal protein HuC/HuD (anti-HuC/D; Clone 16A11; A-21271; Molecular Probes, Eugene, OR, USA; used dilution 1:100), a nuclear marker of immature and mature neurons (Bettini et al., 2016; Iqbal and Byrd-Jacobs, 2010). Anti-TRPC2 is specific against zebrafish antigens. All the other antibodies used in the present study were previously successfully tested on zebrafish olfactory organ by other authors. Incubation of the sections in the secondary antibody was carried out for 1 h 30 min at room temperature: HRP-conjugated goat anti-rabbit IgG (PI-1000; Vector Laboratories, Burlingame, CA, USA; used dilution 1:100) for polyclonal primary antibodies, and HRP-conjugated goat anti-mouse IgG (A4416; Sigma; used dilution 1:100) for monoclonal primary antibody. The immunoreaction was revealed with 0.1 % 3,3-diaminobenzidine (DAB; Sigma) as substrate. Sections were then dehydrated in ethanol, diaphanized in xylene and cover-slipped with Permount (Fisher Scientific, Pittsburgh, PA). Positive controls were obtained from sectioned control fish. Negative controls for the specificity of the immunostaining were realized with 3% normal goat serum as substitution for primary antibodies.

2.5. Image acquisition, quantification and statistical analysis

An Olympus BH-2 microscope (Olympus Italia, Segrate, Italy) equipped with a BEL BlackL 5000 digital camera (BEL Engineering, Monza, Italy) was used as bright-field image acquisition system for tissue sections. All images were obtained in the same light conditions. Adobe Photoshop CS3 (Adobe Systems, San Jose, CA, USA) was employed in micrograph assembly. Image processing, including rotation, resizing (reshaping), addition of bars, letters and symbols, and contrast and brightness adjustment was carried out without content alteration. ImageJ 1.50 g software (https://imagej.nih.gov/ij/) was employed in measurements restricted to the sensory region of lamellae, easily distinguishable from non-sensory regions by their immunostaining pattern. See Lazzari et al. (2017) for details in measurements in the sections treated with the different antibodies.

In sections exposed to anti-calretinin antibody, thickness measurements extended from the epithelial basal lamina to the apical surface, excluding cilia and microvilli. In each section, three epithelial thickness values were calculated from each of three random lamellae and the nine measurements were averaged. Sensory and non-sensory epithelial areas were easily distinguishable due to both presence of long cilia on the surface of non-sensory areas and labelling pattern. The sensory/non-sensory area ratio was calculated in three lamellae per section and averaged.

Physical disector method (Bettini et al., 2016) was employed for evaluating the densities of TrkA-positive cells. In serial pairs of sections, only the cells that appeared in the first section of the pair, but not in the second one, were counted. Cell numbers were evaluated in three lamellae per section using the Cell Counter plugin of ImageJ and averaged.

It was very difficult to count positive cells in anti-G$_{\alpha}$ olf, anti-TRPC2 and anti-HuC/D immunolabeled sections, since anti-G$_{\alpha}$ olf and anti-TRPC2 immunostaining appeared in limited cytoplasmic portions, while anti-HuC/D immunopositive cells were too tightly aggregated. In these conditions, we evaluated the immunostaining intensity by Optical Density (OD), which was estimated as an indirect index of the number of immunopositive cells in a specific lamellar area. Adopting the method of Iqbal and Byrd-Jacobs (2010), the ODs of three lamellae per section were calculated and averaged. Average grey values of sensory regions and background unstained areas of the olfactory lamellae were obtained by ImageJ analysis. Finally, the following formula was ap-plied: OD = log (background grey value/ROI grey value), where ROI is the sensory region of interest.

For each antibody, mean values of fish groups were compared using ANOVA and LSD post hoc test. Data were reported as mean values ± standard errors in bar graphs created by Excel 2013 (Microsoft Corporation, Redmond, WA).

3. Results

None of the three Ni^{2+} ion concentrations used in the present study caused the death of exposed zebrafish. No micro-anatomical effect was observed since olfactory rosettes conserved their overall structure. In the lamellae, tissue disruption, metaplasia and gland modification were not noticed.

In sections stained with anti-calretinin antibody, which marks cell bodies and dendrites of both mature ciliated and microvillar OSNs, the epithelium of the olfactory lamellae is stained from the basal layer to the apical one (Fig. 1a). In the whole olfactory rosette, image analysis revealed that OD of control was statistically greater than OD of each Ni^{2+} ion exposure, whereas, when the three concentrations were compared, ODs of LQ was statistically greater than OD of HQ (Fig. 1b). In the dorsal half of the olfactory rosette, LQ, MQ and HQ values were statistically smaller, but significantly smaller than control values (Fig. 1c). In the ventral half of the rosette, control values are equivalent to LQ ones, but statistically greater than MQ and HQ values. Moreover, LQ values are statistically greater than HQ ones (Fig. 1d). In image analysis, anti-calretinin immunostaining can be used to evaluate other two morphometric parameters: epithelial thickness from the basal la-mina to the free surface and ratio between sensory and non-sensory
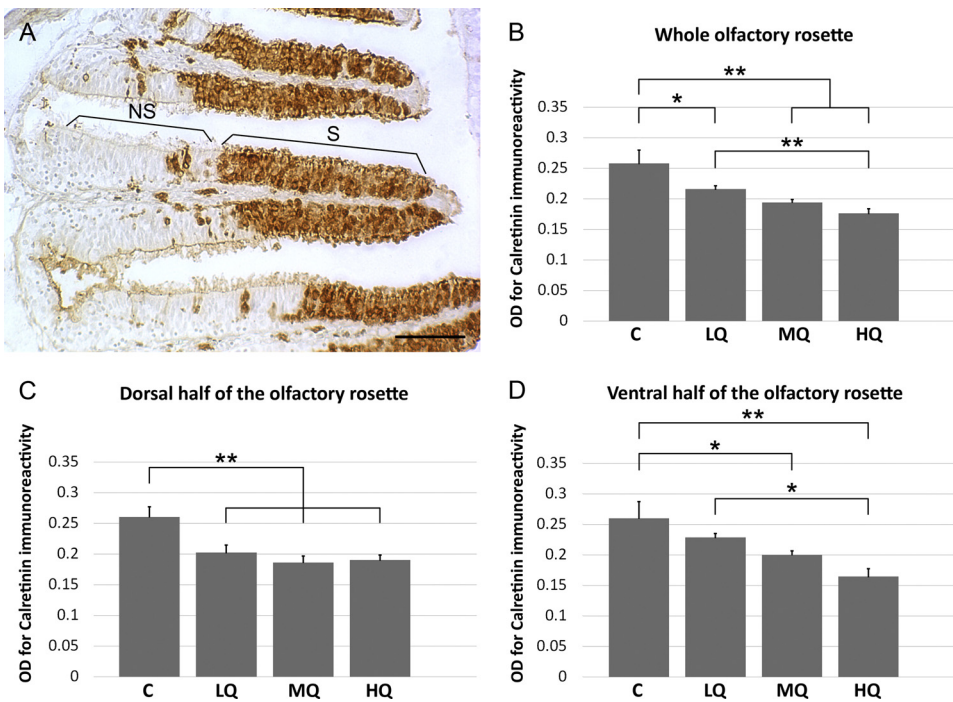
Fig. 1. Calretinin immunohistochemistry in zebrafish olfactory epithelium before and after 0.1, 0.5, and 1 mg L^{-1} Ni^{2+} exposure. A) Heavy anti-calretinin immunoreaction is pre-sent in the sensory area (S) of the olfactory lamellae of control fish. The non-sensory re-gion (NS) of the lamellae is unstained. Scale bar: 50 μm. B) Optical density analysis of the olfactory epithelium in the olfactory rosette. C) Optical density analysis of the olfactory epi-thelium covering lamellae in the dorsal half of the olfactory rosette. D) Optical density ana-lysis of the olfactory epithelium in the lamellae of the ventral portion of the olfactory rosette. C, control, 0 mg L^{-1} Ni^{2+}; LQ, low quantity, 0.1 mg L^{-1} Ni^{2+}; MQ, medium quantity, 0.5 mg L^{-1} Ni^{2+}; HQ, high quantity, 1 mg L^{-1} Ni^{2+}. Asterisks indicate significant differences: *P < 0.05; **P < 0.01.

epithelial areas. After exposure, in the whole olfactory rosette, the thickness of the sensory epithelium was significantly decreased compared to control, but LQ, MQ and HQ values were not statistically different between each other (Fig. 2a). Both dorsal and ventral regions of the rosette showed control thickness to be significantly greater than that of LQ, MQ and HQ, whereas post-exposure values of all are sta-tistically similar (Fig. 2b and c). In the whole olfactory rosette, and in both its dorsal and ventral halves, no significant change in the ratio between sensory and non-sensory areas was observed between the four groups (Fig. 3a–c).

In the OE, anti-G$_{\alpha \text{ olf}}$ antibody stained apical dendrite endings and cilia at the free surface of cOSNs (Fig. 4a). In the whole olfactory ro-sette, the ODs of LQ, MQ and HQ were significantly smaller than those of control, but were statistically equivalent among them (Fig. 4b). The same condition was found in the dorsal half of the rosette (Fig. 4c). The ventral half differed from the dorsal half only in LQ values being sig-nificantly smaller than HQ ones (Fig. 4d).

In the sections treated with anti-TRPC2 antibody, the im-munopositivity was located in the dendritic apical knobs and microvilli of mOSNs (Fig. 5a). In the whole olfactory rosette as well as in both halves of the olfactory rosette, the OD value of control was significantly greater than the values of the three treated groups that were statisti-cally homogeneous when compared between each other (Fig. 5b– d).

Anti-TrkA immunostaining revealed crypt cells, which are big neurons irregularly distributed along the apical zone of the epithelium in the olfactory lamellae (Fig. 6a). The number of crypt cells showed no significant change in the four groups considering either the whole ol-factory rosette or its dorsal and ventral halves (Fig.6b–d).

In the sensory areas of the olfactory lamellae treated with anti-HuC/ D antibody, which is specific for both mature and immature neurons, the olfactory epithelium appeared immunopositive from the basal layer to the apical one (Fig. 7a). In the whole rosette, image analysis showed that ODs of LQ, MQ and HQ were significantly increased compared to control, whereas the values for the three treated groups were statisti-cally uniform (Fig. 7b). In the dorsal half of the olfactory rosette, the four groups were statistically equivalent (Fig. 7c), whereas in the ventral half of the rosette ODs of LQ, MQ and HQ were significantly greater than those of control, as found in the whole organ (Fig. 7d).

Statistical values for all comparisons are reported in supplementary Table S1.

4. Discussion

Immunohistochemistry identifies three main populations of OSNs in the olfactory mucosa of zebrafish. The present study demonstrates that the three populations show differential response to low concentrations of Ni^{2+} ions.

In the whole olfactory rosette, Ni^{2+} induces a significant mean decrease in densitometric values for G$_{\alpha \text{ olf}}$, indicative for cOSNs, of about 46 % compared to control. When compared to each other, the reactions of cOSNs to the three tested concentrations are not statisti-cally different showing that the response of cOSNs is not concentration-dependent, at least for the three concentrations used in the present analysis. When the dorsal and ventral halves of the olfactory rosette are separately examined, Ni^{2+} exposure affects both of them. However, the ventral half shows a greater reduction compared to control than the dorsal half. By comparing these values, we may suppose that in the ventral region of the olfactory rosette cOSNs are more susceptible to Ni^{2+} ions than those in the dorsal one. Moreover, in the ventral half, a concentration-dependent response is present between 0.1 mg L^{-1} and 1 mg L^{-1} Ni^{2+}. Nickel concentrations lower than 0.1 mg L^{-1} would be useful to study, if a concentration-dependency exists also for popula-tions which appear concentration-independent at the lower con-centration used in this study. The reasons and functional significance of this different response are still unclear, but we may hypothesize that subtypes of cOSNs are present in the dorsal and ventral halves of the olfactory rosette. As an alternative, the different sensitivity observed could depend on different water circulation dynamics in the dorsal and ventral part of the rosette. A more intense flow in the ventral region could expose ventral receptors to a greater amount of toxicant.

In Ni^{2+}-treated zebrafish, apical processes immunostained by anti-TRPC2, indicative for mOSNs, are visible on the surface of the olfactory epithelium. Considering the whole olfactory rosette, the densitometric value for anti-TRPC2 shows a statistically significant decrease of about 35% compared to the control. As for cOSNs, no concentration-effect of Ni^{2+} was detected for mOSNs. When dorsal and ventral zones of the olfactory rosette were separately considered, the response for TRPC2 was greater in the ventral half, similarly to what observed for G$_{\alpha \text{ olf}}$.
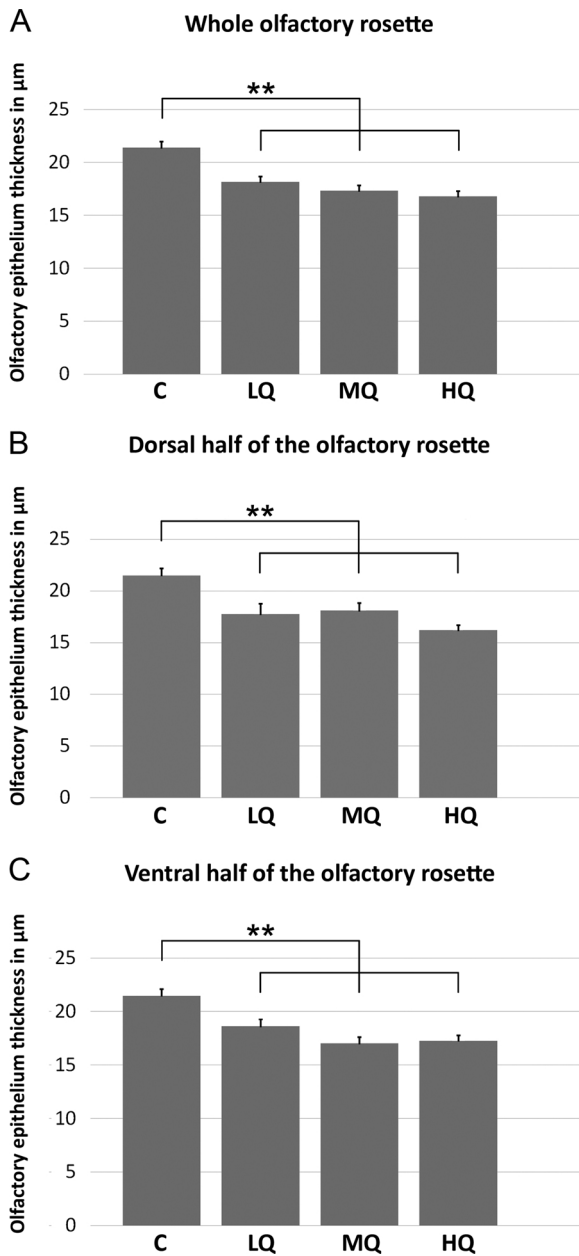
Fig. 2. Calretinin immunohistochemistry in zebrafish olfactory epithelium before and after 0.1, 0.5, and 1 mg L^{-1} Ni^{2+} exposure. A) Sensory epithelium thickness in the lamellae of the olfactory rosette. B) Sensory epithelium thickness in the lamellae of the dorsal zone of the olfactory rosette. C) Sensory epithelium thickness in the lamellae of the ventral zone of the olfactory rosette. C, control, 0 mg L^{-1} Ni^{2+}; LQ, low quantity, 0.1 mg L^{-1} Ni^{2+}; MQ, medium quantity, 0.5 mg L^{-1} Ni^{2+}; HQ, high quantity, 1 mg L^{-1} Ni^{2+}. Asterisks indicate significant differences: **$P < 0.01$.
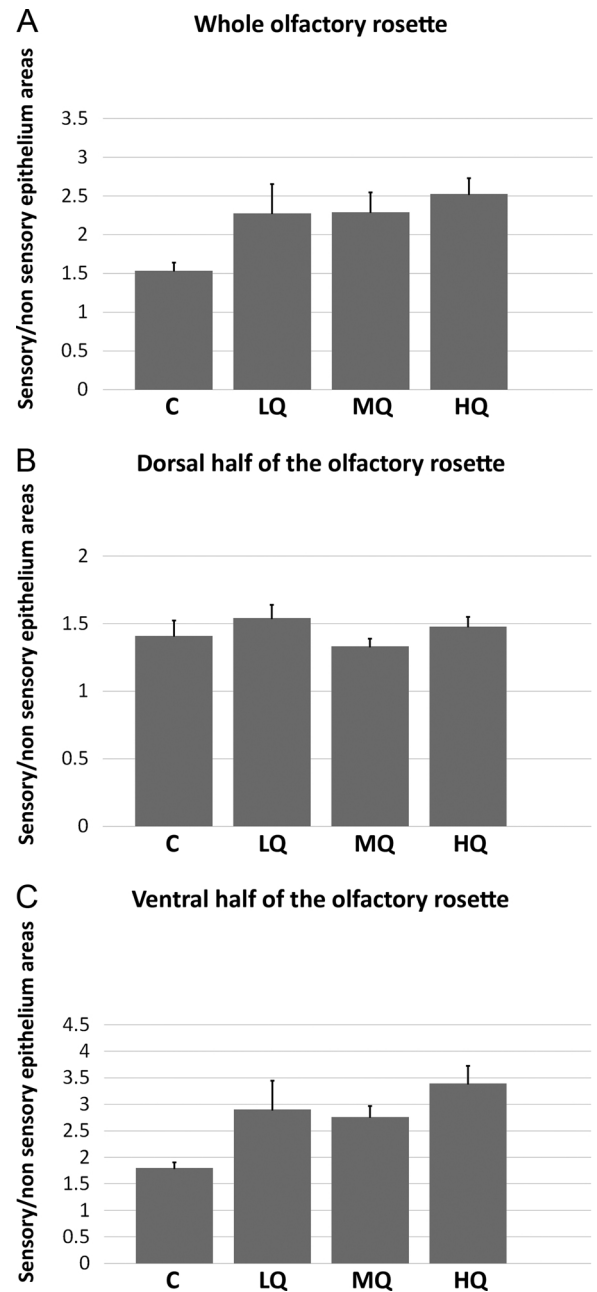

Fig. 3. Calretinin immunohistochemistry in zebrafish olfactory epithelium before and after 0.1, 0.5, and 1 mg L^{-1} Ni^{2+} exposure. A) Ratio between sensory and non-sensory areas of the epithelium overlaying the lamellae in the olfactory rosette. B) Ratio between sensory and non-sensory areas of the epithelium covering the lamellae in the dorsal half of the olfactory rosette. C) Ratio between non-sensory and sensory areas of the epithelium covering the lamellae placed in the ventral half of the olfactory rosette. C, control, 0 mg L^{-1} Ni^{2+}; LQ, low quantity, 0.1 mg L^{-1} Ni^{2+}; MQ, medium quantity, 0.5 mg L^{-1} Ni^{2+}; HQ, high quantity, 1 mg L^{-1} Ni^{2+}.

However, both halves lack a concentration-effect. The ODs for $G_{\alpha \, olf}$ and TRPC2 suggest that cOSNs are more susceptible to Ni^{2+} exposure than mOSNs. Using a functional approach by electro-olfactograms (EOG), Dew et al. (2014) reported that exposure of fathead minnows (*Pimephales promelas*) and yellow perch (*Perca flavescens*) to copper or nickel resulted in differential impairment of OSN classes. However, their data are not in line with the results of the present and a previous histochemical study on zebrafish (Lazzari et al., 2017). Using the specificity of L-alanine to mOSNs and taurocholic acid (TCA) to cOSNs, Dew et al. (2014) reported that in both species nickel (50, 100, or 500 µg L^{-1} of Ni^{2+}) caused impairment of mOSN but had no effect on cOSNs. On the contrary, low Cu^{2+} concentrations affected only cOSNs.

Our results in zebrafish contradict EOG outcomes. Nonetheless, also EOG studies show some discrepancies between each other. In fact, in previous electro-olfactographic studies on coho salmon (*Oncorhynchus kisutch*), copper impaired the response to TCA but also to L-serine (Baldwin et al., 2003; Sandahl et al., 2007). As pointed out by Dew et al., (2012), Dew et al., (2014), it has to be considered that different technical strategies, exposure times, ion concentrations, water chemistry, and inherent differences among species could account for the differences in electrophysiological studies.
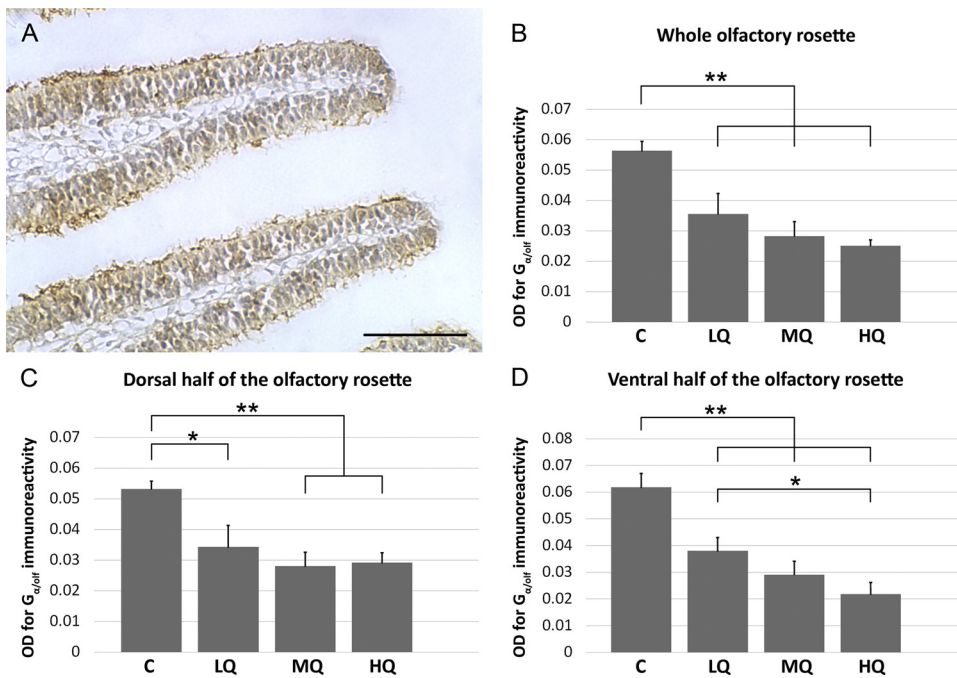
Fig. 4. $G_{\alpha\,olf}$ immunohistochemistry in zebrafish olfactory epithelium before and after 0.1, 0.5, and 1 mg L^{-1} Ni^{2+} treatment. A) In the olfactory lamellae of control fish, the receptor cell knobs located in the superficial zone of the sensory epithelium show different Gα olf immunostaining intensity. Scale bar: 50 μm. B) Optical density analysis of the olfactory epithelium surface in the whole olfactory rosette. C) Optical density analysis of the olfactory epithelium surface in the lamellae of the dorsal region of the olfactory rosette. D) Optical density analysis of the sensory epithelial surface in the lamellae of the ventral zone of the olfactory rosette. C, control, 0 mg L^{-1} Ni^{2+}; LQ, low quantity, 0.1 mg L^{-1} Ni^{2+}; MQ, medium quantity, 0.5 mg L^{-1} Ni^{2+}; HQ, high quantity, 1 mg L^{-1} Ni^{2+}. Asterisks indicate significant differences: *$P < 0.05$; **$P < 0.01$.

The effect of metals on the different OSN populations of fish was also studied by histological techniques. Kolmakov et al. (2009) reported the specific activity of copper on cOSNs of goldfish. In an immunohistochemical study on olfactory rosettes of zebrafish (Lazzari et al., 2017), we found that low concentration of Cu^{2+} affected both cOSNs and mOSNs but to different extent. We reported that the OD for $G_{\alpha\,olf}$ decreased by about 60% compared to control, whereas the OD for TRPC2 decreased by about 30%. Therefore, in our immunohistochemical study, cOSNs appear more susceptible, about twice as sensitive, to Cu^{2+} than mOSNs. In the present study, Ni^{2+} exposure resulted in a mean reduction in $G_{\alpha\,olf}$ OD by about 46% compared to control, whereas the TRPC2 OD decreased by about 35%. The present and previous immunohistochemical studies on zebrafish (Lazzari et al.,

2017) do not support a specific activity of copper on cOSNs and of nickel on mOSNs, as reported by Dew et al. (2014) in fathead minnow and yellow perch. In zebrafish, we found that both Cu^{2+} and Ni^{2+} exposures affect cOSNs and mOSNs, and these metals have greater ef-fects on cOSNs (Lazzari et al., 2017 and the present study).

Since densitometric analysis reveals a decrement in immunostaining intensity only at the level of the apical processes of OSNs, this may represent an indirect evidence of the reduction in the number of OSNs, and consequently be suggestive of cell death. However, both a reduction in the number of apical processes and a drop in the expression of the stained proteins may account for OD decrement. In a scanning electron microscopy study on the ultrastructure of the apical surface of zebrafish olfactory epithelium, Ghosh and Mandal (2014) found that
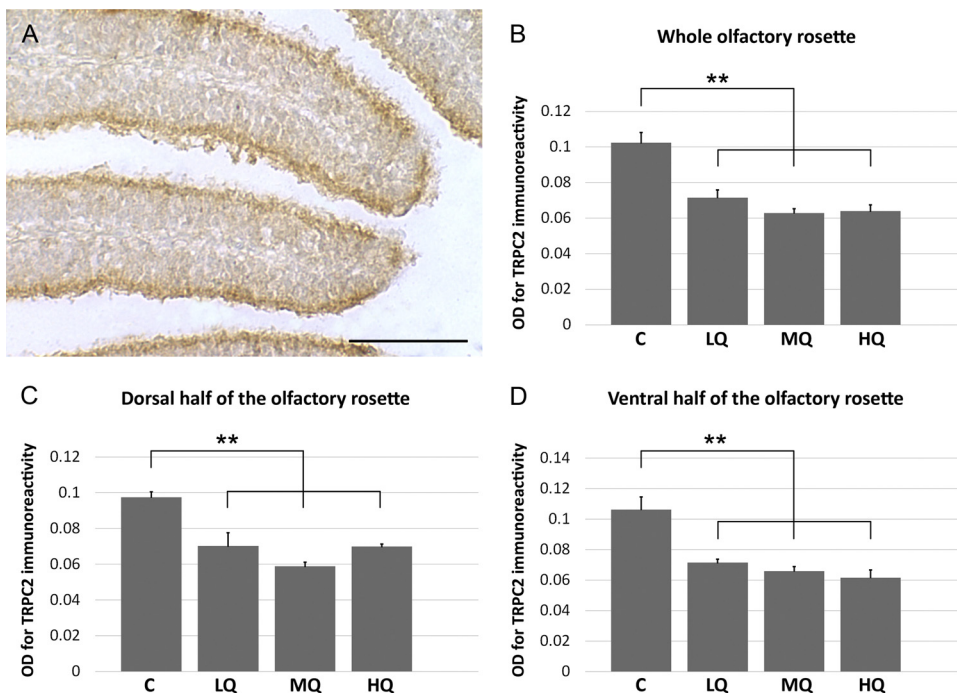

Fig. 5. TRPC2 immunohistochemistry in zebrafish olfactory epithelium before and after 0.1, 0.5, and 1 mg L^{-1} Ni^{2+} exposure. A) In the sensory areas of the olfactory lamellae of control fish, the apical region of the olfactory epithelium contains the receptor cell endings, which are stained by anti-TRPC2 antibody. Scale bar: 50 μm. B) Optical density analysis of the olfactory epithelium surface in the whole olfactory rosette. C) Optical density analysis of the olfactory epithelium surface in the lamellae of the dorsal half of the olfactory rosette. D) Optical density analysis of the olfactory epithelium surface in the lamellae of the ventral half of the olfactory rosette. C, control, 0 mg L^{-1} Ni^{2+}; LQ, low quantity, 0.1 mg L^{-1} Ni^{2+}; MQ, medium quantity, 0.5 mg L^{-1} Ni^{2+}; HQ, high quantity, 1 mg L^{-1} Ni^{2+}. Asterisks indicate significant differences: **$P < 0.01$.
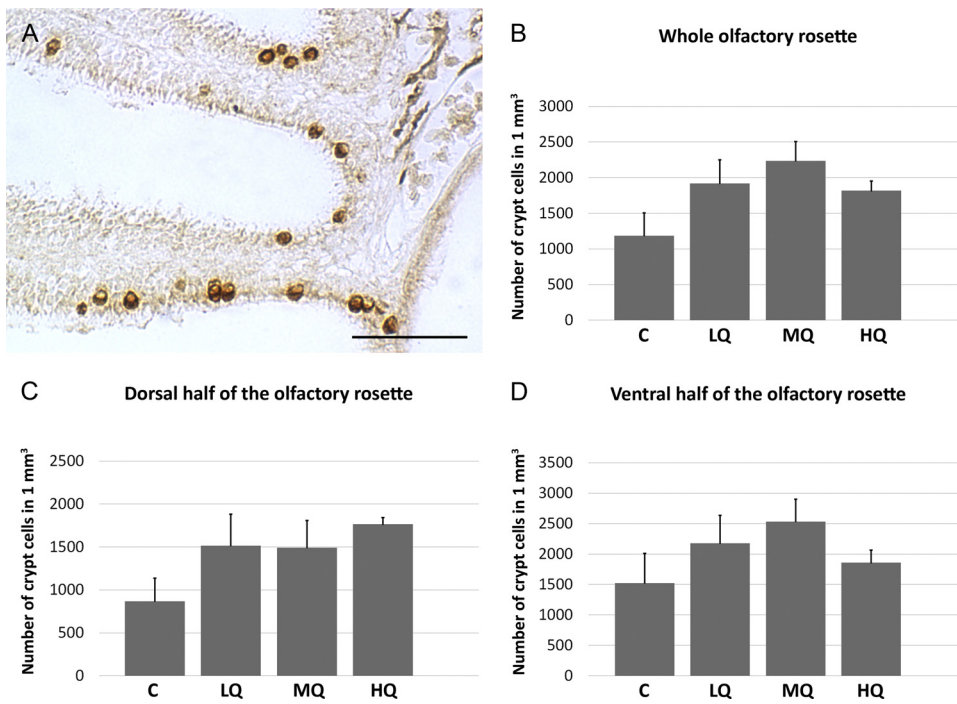
Fig. 6. TrkA immunohistochemistry in zebrafish olfactory epithelium before and after 0.1, 0.5, and 1 mg L^{-1} Ni^{2+} treatment. A) In olfactory lamellae of control fish, immunostained crypt cells appear in the superficial layer of the sensory area. Scale bar: 50 μm. B) Density of crypt cells in lamellae of the whole olfactory rosette. C) Density of crypt cells in lamellae of the dorsal zone of the olfactory rosette. D) Density of crypt cells in lamellae of the ventral zone of the olfactory rosette. C, control, 0 mg L^{-1} Ni^{2+}; LQ, low quantity, 0.1 mg L^{-1} Ni^{2+}; MQ, medium quantity, 0.5 mg L^{-1} Ni^{2+}; HQ, high quantity, 1 mg L^{-1} Ni^{2+}.

Zn^{2+} exposure led to the loss of cilia, similarly to Cu^{2+} exposure (Kolmakov et al., 2009), with the retention of microvilli. However, at present, ultrastructural studies on fish olfactory epithelium exposed to Ni^{2+} ions are absent. This kind of studies might reveal, whether ion exposure results in OSN death rather than cilia and/or microvilli reduction. In our histological test, cilia are still clear in the apical surface of the exposed olfactory epithelium. Therefore, a reduction in $G_{\alpha\ olf}$ and TRPC2 expressions may be supposed. According to Tilton et al., (2008), Tilton et al., (2011) and Wang et al. (2013b), Cu^{2+} exposure could result in a decrease in antigen expression without morphology alteration and death of OSNs. However, our morphometric analysis revealed a reduction in epithelial thickness, so we hypothesize that the

differences in the OD values following Ni^{2+} exposure could be more likely related to cell death, as we suggested also for Cu^{2+} exposure (Lazzari et al., 2017).

Crypt cells are an additional cell population of OSNs present in the olfactory epithelium of fish (Ferrando et al., 2006; Gayoso et al., 2011, 2012; Hansen and Finger, 2000; Hansen and Zeiske, 1998; Lazzari et al., 2007). S100 was the molecular marker initially used in the histochemical identification of crypt cells (Braubach et al., 2012; Germanà et al., 2004; Sato et al., 2005). However, S100 can immunodetect other cell types in addition to crypt cells (Bettini et al., 2017; Germanà et al., 2004; Oka et al., 2012; Sato et al., 2005). Therefore, S100 is now considered non-specific (Ahuja et al., 2013; Bettini et al., 2017). TrkA,
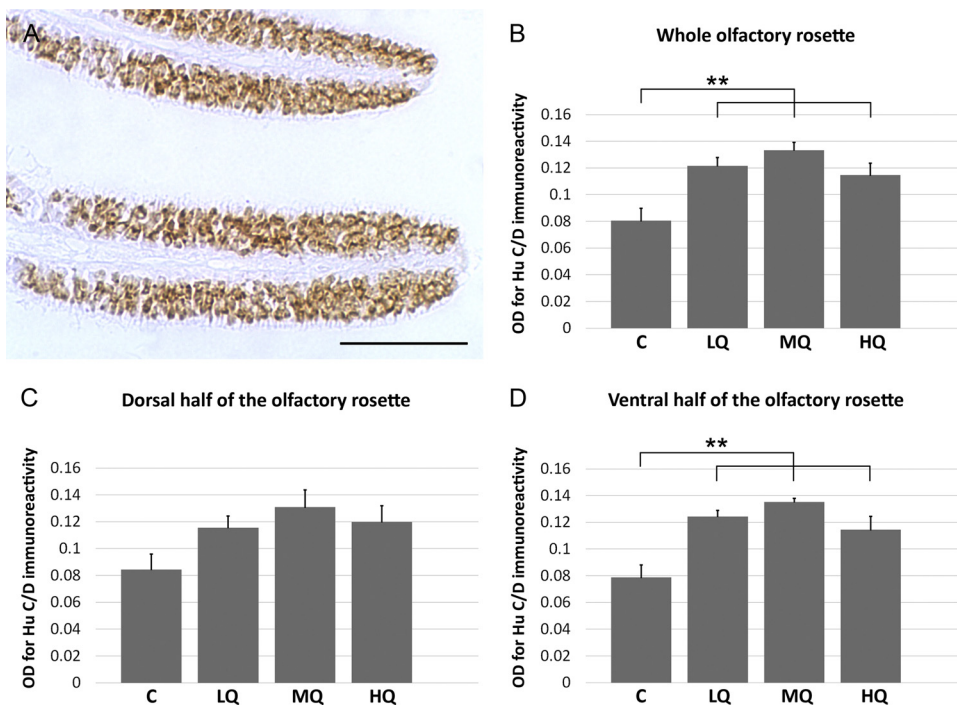

Fig. 7. HuC/D immunohistochemistry in zebrafish olfactory epithelium before and after 0.1, 0.5, and 1 mg L^{-1} Ni^{2+} treatment. A) In control fish, all the neurons located in the sensory regions of the olfactory lamellae show clear immunopositive cell bodies. Scale bar: 50 μm. B) Optical density analysis of the olfactory epithelium covering lamellae in the olfactory rosette. C) Optical density analysis of the olfactory epithelium in the dorsal half of the olfactory rosette. D) Optical density analysis of the olfactory epithelium in the ventral half of the olfactory rosette. C, control, 0 mg L^{-1} Ni^{2+}; LQ, low quantity, 0.1 mg L^{-1} Ni^{2+}; MQ, medium quantity, 0.5 mg L^{-1} Ni^{2+}; HQ, high quantity, 1 mg L^{-1} Ni^{2+}. Asterisks indicate significant differences: **P < 0.01.

originally used by Catania et al. (2003), has proven to be a strong and specific marker for crypt cells in zebrafish (Ahuja et al., 2013; Bettini et al., 2016). Therefore, in our studies on the effect of heavy metals on zebrafish olfaction (Lazzari et al., 2017 and the present study), we employed anti-TrkA to detect crypt cells. The effect of Ni^{2+} exposure on crypt cells resembles that observed following Cu^{2+} treatment (Lazzari et al., 2017). Although in both studies cell count could have drawn attention to a possible increment in crypt cell population after metal exposure, statistical analysis does not support it, neither compared to control, nor when the comparison is done between the different tested ion concentrations. Therefore, we can conclude that Cu^{2+} and Ni^{2+} exposures do not seem to affect crypt cells (Lazzari et al., 2017 and the present study). The specific morphology of crypt cells can explain this result (Lazzari et al., 2007). In cOSNs and mOSNs, cilia and microvilli originating from the dendritic apical region of the sensory neurons are directly exposed to the outer aquatic environment at the surface of the olfactory lamellae. This may increase susceptibility of cilia and microvilli to water contaminants. In crypt cells both cilia and microvilli are present, but they are not directly exposed to surrounding water. Instead, they are contained in a deep cavity located in the apical region of the cell. This crypt opens to the outer environment through a narrow hole, allowing for a limited passage of substances, including metal ions. In crypt cells, this position of cilia and flagella, enclosed in the crypt, may account for their protection.

In the OE of vertebrates, mitotic proliferation and subsequent cell differentiation occur throughout the life in order to substitute dead OSNs (Bettini et al., 2006a; Graziadei and Monti Graziadei, 1979). In the physiological state, mature OSNs downregulate proliferation and differentiation of new sensory cells to maintain their population size at a stable level (Wu et al., 2003). Following Ni^{2+} exposure, the increase in the OD for HuC/D, indicative for total neuronal population including undifferentiated neurons, together with the observed reduction in the OD for $G_{\alpha\ olf}$ and TRPC2, seems to confirm that a certain degree of cell death takes place in the populations of mature OSNs with concomitant growth in the number of immature neurons. Statistical analysis shows that the increase in HuC/D OD is not dependent on metal ion concentration. When dorsal and ventral halves of the olfactory rosettes are separately considered, participation of undifferentiated neurons appears statistically significant in the ventral region. This is in agreement with the observation that Ni^{2+} exposure causes a greater reduction in both anti-$G_{\alpha\ olf}$ and anti-TRPC2 ODs in the ventral region compared to the dorsal half. This confirms that undifferentiated neurons responsible for neuronal restoration in the olfactory epithelium are present in the ventral portion of the olfactory rosette, the region where damage appears greater.

In our study on zebrafish olfactory organ, Ni^{2+} exposure does not cause other recognizable effects in addition to those revealed by image analysis. In particular, during exposure time, no fish died, confirming the sub-lethal nature of the tested concentrations. Swimming and feeding behaviors appeared unchanged. The olfactory rosettes and lamellae conserved their structure, in agreement with the results of previous studies on the effects of 30 µg L^{-1} Cu^{2+} in zebrafish (Lazzari et al., 2017) and 20 µg L^{-1} Cu^{2+} in *Tilapia mariae* (Bettini et al., 2006b). On the contrary, 40 µg L^{-1} Cu^{2+} caused clear alterations in the olfactory epithelium of *Tilapia* (Bettini et al., 2006b). Ultrastructural studies have revealed Cu^{2+}-dependent alterations also in goldfish OSNs (Kolmakov et al., 2009). However, at present, there is no information on the ultrastructural reaction of cOSNs and mOSNs after Ni^{2+} ex-posure. New ultrastructural studies could provide useful information to explain whether Ni^{2+} exposure results in cell death and/or in loss of cilia and microvilli.

In the present study, the reduction in the OD for calretinin (marker for a heterogeneous population of mature c- and mOSNs) is in agreement with the decrease in the ODs for $G_{\alpha\ olf}$ and TRPC2. In particular, when the dorsal and ventral halves of the olfactory rosette are separately considered, the latter shows a greater calretinin OD reduction

and a concentration-dependent effect consistent with $G_{\alpha\ olf}$ behavior.

In the olfactory epithelium, OSNs are associated with non-neuronal cells. The effects of Cu^{2+} exposure on these non-neuronal cells are considered to be lower than the effects on OSNs (Julliard et al., 1993, 1996; Moran et al., 1992). At present, there is no evidence on the response of fish non-neuronal cells to Ni^{2+} exposure. However, the reduction in epithelial thickness more likely depends on the decline in the number of c- and mOSNs.

In a previous immunohistochemical study on zebrafish, exposure to 30 µg L^{-1} Cu^{2+} caused an increase in the sensory area compared to control (Lazzari et al., 2017). The increase was faster in the lamellae of the ventral half of the olfactory rosette and corresponded to histological recovery of the olfactory epithelium. This increase of the sensory area appears to be related to functional recovery, as suggested by behavioral and electrophysiological analysis after Cu^{2+} exposure in two different species, Colorado pikeminnow (*Ptychocheilus lucius*) (Beyers and Farmer, 2001) and fathead minnow (*Pimephales promelas*) (Dew et al., 2012). We did not observe any increase in the sensory area of zebrafish during Ni^{2+} treatment. However, new, dedicated studies could address neuronal recovery after Ni^{2+} exposure.

5. Conclusions

The different markers used in this immunohistochemical study provide convergent results on the reaction of zebrafish OSNs to Ni^{2+} exposure. In particular, the present analysis shows that the different classes of OSNs have different responses to nickel ion exposure at sublethal concentrations. Ciliated OSNs appear the most sensitive with some concentration-dependent effects. Microvillous OSNs show weaker reaction without concentration-dependent effects in the range of concentration utilized. Crypt cells show no statistically significant modification after Ni^{2+} exposure. Other studies focused on specific metal ions suggested cOSNs as more susceptible than mOSNs (Dew et al., 2014; Ghosh and Mandal, 2014; Kolmakov et al., 2009; Lazzari et al., 2017; present study).

In the ventral half of the olfactory rosette, olfactory lamellae appear more susceptible to metal than dorsal lamellae. Differences in the activities of olfactory receptors may account for this diversity and are under investigation. Alsop and Wood (2011), Alsop and Wood (2013) proposed that the toxicity following metal exposure is the result of total ion loss, especially Na^+, rather than the disruption of ion uptake, as previously suggested. Several studies ascribed different functions to cOSNs, mOSNs and crypt cells (Ahuja et al., 2013; Bazáes and Schmachtenberg, 2012; Biechl et al., 2016; Hamdani and Døving, 2006; Sato and Suzuki, 2001; Vielma et al., 2008). Other studies pointed out behavioral effects of metal exposure: most of them focused on Cu^{2+} (da Silva Acosta et al., 2016; Poulsen et al., 2014; Scott and Sloman, 2004; Simonato et al., 2016; Sovová et al., 2014; Svecevičius, 2012; Tilton et al., 2011), few on Ni^{2+} (Dew et al., 2014, Dew et al., 2016).

Immunohistochemical results provide novel information on changes in OSN composition and/or molecular marker expression. However, to understand how the overall olfactory sensing is affected, additional studies with electrophysiological measurements and behavioral tests will address the effect of nickel pollution on fish olfaction. It would also be worth considering the possibility that long exposures to sublethal concentrations may also have effects on other cells involved in sensory integration and final response to stimuli. Moreover, at present, no substance has been recognized as specific activator of crypt cells, making the experimental set up for this kind of studies not straight-forward.

Further histochemical, electrophysiological and behavioral studies on fish olfaction will be fundamental to understand how the contamination of aquatic systems affects fish populations resulting in population decline with environmental and socio-economic outcomes.

Appendix A. Supplementary data

Supplementary material related to this article can be found, in the online version, at doi:https://doi.org/10.1016/j.aquatox.2018.10.011.

References

Ahuja, G., Ivandić, I., Saltürk, M., Oka, Y., Nadler, W., Korsching, S.I., 2013. Zebrafish crypt neurons project to a single, identified mediodorsal glomerulus. Sci. Rep. 3, 2063. https://doi.org/10.1038/srep02063.

Alam, N., Corbett, S.J., Ptolemy, H.C., 2008. Environmental health risk assessment of nickel contamination of drinking water in a country town in NSW. NSW Public Health Bull. 19, 170–173. https://doi.org/10.1071/NB97043.

Alsop, D., Wood, C.M., 2011. Metal uptake and acute toxicity in zebrafish: Common mechanisms across multiple metals. Aquat. Toxicol. 105, 385–393. https://doi.org/10.1016/j.aquatox.2011.07.010.

Alsop, D., Wood, C.M., 2013. Metal and pharmaceutical mixtures: Is ion loss the mechanism underlying acute toxicity and widespread additive toxicity in zebrafish? Aquat. Toxicol. 140-141, 257–267. https://doi.org/10.1016/j.aquatox.2013.05.021.

Azizishirazi, A., Dew, W.A., Forsyth, H.L., Pyle, G.G., 2013. Olfactory recovery of wild yellow perch from metal contaminated lakes. Ecotoxicol. Environ Saf. 88, 42–47. https://doi.org/10.1016/j.ecoenv.2012.10.015.

Baldwin, D.H., Sandahl, J.F., Labenia, J.S., Scholz, N.L., 2003. Sublethal effects of copper on coho salmon: impacts on nonoverlapping receptor pathways in the peripheral olfactory nervous system. Environ. Toxicol. Chem. 22, 2266–2274.

Baldwin, D.H., Tatara, C.P., Scholz, N.L., 2011. Copper-induced olfactory toxicity in salmon and steelhead: extrapolation across species and rearing environments. Aquat. Toxicol. 101 (2011), 295–297. https://doi.org/10.1016/j.aquatox.2010.08.011.

Bazáes, A., Schmachtenberg, O., 2012. Odorant tuning of olfactory crypt cells from juvenile and adult rainbow trout. J. Exp. Biol. 215, 1740–1748. https://doi.org/10.1242/jeb.067264.

Bettini, S., Ciani, F., Franceschini, V., 2006a. Cell proliferation and growth-associated protein 43 expression in the olfactory epithelium in Poecilia reticulata after copper solution exposure. Eur. J. Histochem. 50, 141–146.

Bettini, S., Ciani, F., Franceschini, V., 2006b. Recovery of the olfactory receptor neurons in the African Tilapia mariae following exposure to low copper level. Aquat. Toxicol. 76, 321–328. https://doi.org/10.1016/j.aquatox.2005.10.009.

Bettini, S., Lazzari, M., Ferrando, S., Gallus, L., Franceschini, V., 2016. Histopathological analysis of the olfactory epithelium of zebrafish (Danio rerio) exposed to sublethal doses of urea. J. Anat. 228, 59–69. https://doi.org/10.1111/joa.12397.

Bettini, S., Milani, L., Lazzari, M., Maurizii, M.G., Franceschini, V., 2017. Crypt cell markers in the olfactory organ of Poecilia reticulata: analysis and comparison with the fish model Danio rerio. Brain Struct Funct 222, 3063–3074. https://doi.org/10.1007/s00429-017-1386-2.

Beyers, D.W., Farmer, M.S., 2001. Effects of copper on olfaction of colorado pikeminnow. Environ. Toxicol. Chem. 20, 907–912.

Biechl, D., Tietje, K., Gerlach, G., Wullimann, M.F., 2016. Crypt cells are involved in kin recognition in larval zebrafish. Sci. Rep. 6, 24590. https://doi.org/10.1038/srep24590.

Bondier, J.R., Michel, G., Propper, A., Badot, P.M., 2008. Harmful effects of cadmium on olfactory system in mice. Inhal. Toxicol. 20, 1169–1177. https://doi.org/10.1080/08958370802207292.

Boran, H., Şaffak, S., 2018. Comparison of dissolved nickel and nickel nanoparticles toxicity in larval zebrafish in terms of gene expression and DNA damage. Arch. Environ. Contam. Toxicol. 74, 193–202. https://doi.org/10.1007/s00244-017-0468-8.

Braubach, O.R., Fine, A., Croll, R.P., 2012. Distribution and functional organization of glomeruli in the olfactory bulbs of zebrafish (Danio rerio). J. Comp. Neurol. 520, 2317–2339. https://doi.org/10.1002/cne.23075.

Calderón-Garcidueñas, L., 2015. Influence of toxins on olfactory function and their potential association with neurodegenerative disease. In: Doty, R.L. (Ed.), Handbook of olfaction and gustation. Wiley and Son, Hoboken,NJ, pp. 485–512. https://doi.org/10.1002/9781118971758.ch20.

Cardwell, R.D., Foreman, D.G., Payne, T.R., Wilbur, D.J., 1976. Acute toxicity of selenium dioxide to freshwater fishes. Arch. Environ. Contam. Toxicol. 4, 129–144.

Catania, S., Germanà, A., Laurà, R., Gonzalez-Martinez, T., Ciriaco, E., Vega, J.A., 2003. The crypt neurons in the olfactory epithelium of the adult zebrafish express TrkA-like immunoreactivity. Neurosci. Lett. 350, 5–8. https://doi.org/10.1016/S0304-3940(03)00751-1.

Chua, E.M., Flint, N., Wilson, S.P., Vink, S., 2018. Potential for biomonitoring metals and metalloids using fish condition and tissue analysis in an agricultural and coal mining region. Chemosphere 202, 598–608. https://doi.org/10.1016/j.chemosphere.2018.03.080.

da Silva Acosta, D., Danielle, N.M., Altenhofen, S., Luzardo, M.D., Gomes Costa, P., Bianchini, A., Bonan, C.D., Souza da Silva, R., Dafre, A.L., 2016. Copper at low levels impairs memory of adult zebrafish (Danio rerio) and affects swimming performance of

larvae. Comp. Biochem. Physiol. C Toxicol. Pharmacol 185-186, 122–130. https://doi.org/10.1016/j.cbpc.2016.03.008.

Dew, W.A., Wood, C.M., Pyle, G.G., 2012. Effects of continuous copper exposure and calcium on the olfactory response of fathead minnows. Environ. Sci. Technol. 46, 9019–9026. https://doi.org/10.1021/es300670p.

Dew, W.A., Azizishirazi, A., Pyle, G.G., 2014. Contaminant-specific targeting of olfactory sensory neuron classes: connecting neuron class impairment with behavioural deficits. Chemosphere 112, 519–525. https://doi.org/10.1016/j.chemosphere.2014.02.047.

Dew, W.A., Veldhoen, N., Carew, A.C., Helbing, C.C., Pyle, G.G., 2016. Cadmium-induced olfactory dysfunction in rainbow trout: Effects of binary and quaternary metal mixtures. Aquat. Toxicol. 172, 86–94. https://doi.org/10.1016/j.aquatox.2015.12.018. Døving, K.B., Hansson, K.A., Backstrom, T., Hamdani, E.H., 2011. Visualizing a set of olfactory sensory neurons responding to a bile salt. J. Exp. Biol. 214, 80–87. https://doi.org/10.1242/jeb.046607.

Eisthen, H.L., 1992. Phylogeny of the vomeronasal system and of receptor cell types in the olfactory and vomeronasal epithelia of vertebrates. Microsc. Res. Tech. 23, 1–21. https://doi.org/10.1002/jemt.1070230102.

Ferrando, S., Bottaro, M., Gallus, L., Girosi, L., Vacchi, M., Tagliafierro, G., 2006. Observations of crypt neuron-like cells in the olfactory epithelium of a cartilaginous fish. Neurosci. Lett. 403, 280–282. https://doi.org/10.1016/j.neulet.2006.04.056.

Ferrando, S., Bottaro, M., Gallus, L., Girosi, L., Vacchi, M., Tagliafierro, G., 2007. First detection of olfactory marker protein (OMP) immunoreactivity in the olfactory epithelium of a cartilaginous fish. Neurosci. Lett. 413, 173–176. https://doi.org/10.1016/j.neulet.2006.11.051.

Ferrando, S., Gallus, L., Gambardella, C., Amaroli, A., Vallarino, M., Tagliafierro, G., 2011. Immunolocalization of G protein alpha subunits in the olfactory system of Polypterus senegalus (Cladistia, Actinopterygii). Neurosci. Lett. 499, 127–131. https://doi.org/10.1016/j.neulet.2011.05.052.

Gayoso, J.Á., Castro, A., Anadón, R., Manso, M.J., 2011. Differential bulbar and extrabulbar projections of diverse olfactory receptor neuron populations in the adult zebrafish (Danio rerio). J. Comp. Neurol. 519, 247–276. https://doi.org/10.1002/cne.22518.

Gayoso, J., Castro, A., Anadón, R., Manso, M.J., 2012. Crypt cells of the zebrafish Danio rerio mainly project to the dorsomedial glomerular field of the olfactory bulb. Chem. Senses 37, 357–369. https://doi.org/10.1093/chemse/bjr109.

Germanà, A., Montalbano, G., Laurà, R., Ciriaco, E., del Valle, M.E., Vega, J.A., 2004. S100 protein-like immunoreactivity in the crypt olfactory neurons of the adult zebrafish. Neurosci. Lett. 371, 196–198. https://doi.org/10.1016/j.neulet.2004.08.077.

Germanà, A., Paruta, S., Germanà, G.P., Ochoa-Erena, F.J., Montalbano, G., Vega, J.A., 2007. Differential distribution of S100 protein and calretinin in mechanosensory and chemosensory cells of adult zebrafish (Danio rerio). Brain Res. 1162, 48–55. https://doi.org/10.1016/j.brainres.2007.05.070.

Ghosh, D., Mandal, D.K., 2014. Mercuric chloride induced toxicity responses in the olfactory epithelium of Labeo rohita (Hamilton): A light and electron microscopy study. Fish Physiol. Biochem. 40, 83–92. https://doi.org/10.1007/s10695-013-9826-2.

Giattina, J.D., Garton, R.R., Stevens, D.G., 1982. Avoidance of copper and nickel by rainbow trout Salmo gairdneri as monitored by a computer based data acquisition system. Trans. Amer. Fish. Soc. 111, 491–504. https://doi.org/10.1577/1548-8659(1982)111 < 491:AOCANB > 2.0.CO;2.

Graziadei, P.P.C., Monti Graziadei, G.A., 1979. Neurogenesis and neuron regeneration in the olfactory system of mammals. I. Morphological aspects of differentiation and structural organization of the olfactory sensory neurons. J. Neurocytol. 8, 1–18. Hamdani, H., Døving, K.B., 2006. Specific projection of the sensory crypt cells in the olfactory system in crucian carp, Carassius carassius. Chem. Senses 31, 63–67. https://doi.org/10.1093/chemse/bjj006.

Hamdani, E.H., Døving, K.B., 2007. The functional organization of the fish olfactory system. Prog. Neurobiol. 82, 80–86. https://doi.org/10.1016/j.pneurobio.2007.02.007.

Hansen, A., Finger, T.E., 2000. Phyletic distribution of crypt-type olfactory receptor neurons in fishes. Brain Behav. Evol. 55, 100–110. https://doi.org/10.1159/000006645.

Hansen, A., Rolen, S.H., Anderson, K., Morita, Y., Caprio, J., Finger, T.E., 2003. Correlation between olfactory receptor cell type and function in the channel catfish. J. Neurosci. 23, 9328–9339.

Hansen, A., Zeiske, E., 1998. The peripheral olfactory organ of the zebrafish, Danio rerio: an ultrastructural study. Chem. Senses 23 (1), 39–48. https://doi.org/10.1093/chemse/23.1.39.

Hentig, J.T., Byrd-Jacobs, C.A., 2016. Exposure to zinc sulfate results in differential effects on olfactory sensory neuron subtypes in adult zebrafish. Int. J. Mol. Sci. 17, 1445. https://doi.org/10.3390/ijms17091445.

Hill, A.J., Teraoka, H., Heideman, W., Peterson, R.E., 2005. Zebrafish as a model vertebrate for investigating chemical toxicity. Toxicol. Sci. 86, 6–19. https://doi.org/10.1093/toxsci/kfi110.

Iqbal, T., Byrd-Jacobs, C., 2010. Rapid degeneration and regeneration of the zebrafish olfactory epithelium after Triton X-100 application. Chem. Senses 35, 351–361. https://doi.org/10.1093/chemse/bjq019.

Julliard, A.K., Saucier, D., Astic, L., 1993. Effects of chronic lowlevel copper exposure on ultrastructure of the olfactory system in rainbow trout (Oncorhynchus mykiss). Histol. Histopathol. 8, 665–672.

Julliard, A.K., Saucier, D., Astic, L., 1996. Time-course of apoptosis in the olfactory epithelium of rainbow trout exposed to a low copper level. Tissue Cell 28, 367–377. https://doi.org/10.1016/S0040-8166(96)80023-1.

Katagi, T., 2010. Bioconcentration, bioaccumulation, and metabolism of pesticides in aquatic organisms. Rev. Environ. Contam. Toxicol. 204, 1–132. https://doi.org/10.1007/978-1-4419-1440-8_1.

Klečka, G., Persoon, C., Currie, R., 2010. Chemicals of emerging concern in the great lakes basin: an analysis of environmental exposures. In: In: Whitacre, D.M. (Ed.), Reviews of Environmental Contamination and Toxicology, vol. 207. Springer, New York, pp. 1–93. https://doi.org/10.1007/978-1-4419-6406-9_1.

Kollár, T., Kása, E., Ferincz, A., Urbányi, B., Csenki-Bakos, Z., Ákos Horváth, A., 2018. Development of an in vitro toxicological test system based on zebrafish (*Danio rerio*) sperm analysis. Environ. Sci. Pollut. Res. 1–11. https://doi.org/10.1007/s11356-018-1613-2.

Kolmakov, N.N., Hubbard, P.C., Lopes, O., Canario, A.V., 2009. Effect of acute copper sulfate exposure on olfactory responses to amino acids and pheromones in goldfish *(Carassius auratus)*. Environ. Sci. Technol. 43, 8393–8399. https://doi.org/10.1021/es901166m.

Laberge, F., Hara, T.J., 2001. Neurobiology of fish olfaction: a review. Brain Res. Rev. 36, 46–59.

Laframboise, A.J., Zielinski, B.S., 2011. Responses of round goby (*Neogobius melanostomus*) olfactory epithelium to steroids released by reproductive males. J. Comp. Physiol. A. 197, 999–1008. https://doi.org/10.1007/s00359-011-0662-5.

Lammer, E., Carr, G.J., Wendler, K., Rawlings, J.M., Belanger, S.E., Braunbeck, T., 2009a. Is the fish embryo toxicity test (FET) with the zebrafish (*Danio rerio*) a potential alternative for the fish acute toxicity test? Comp. Biochem. Physiol. C Toxicol. Pharmacol. 149, 196–209. https://doi.org/10.1016/j.cbpc.2008.11.006.

Lammer, E., Kamp, H.G., Hisgen, V., Koch, M., Reinhard, D., Salinas, E.R., Wendler, K., Zok, S., Braunbeck, T., 2009b. Development of a flow-through system for the fish embryo toxicity test (FET) with the zebrafish (*Danio rerio*). Toxicol. In Vitro 23, 1436–1442. https://doi.org/10.1016/j.tiv.2009.05.014.

Lari, E., Bogart, S.J., Pyle, G.G., 2018. Fish can smell trace metals at environmentally relevant concentrations in freshwater. Chemosphere 203, 104–108. https://doi.org/10.1016/j.chemosphere.2018.03.174.

Lazzari, M., Bettini, S., Ciani, F., Franceschini, V., 2007. Light and transmission electron microscopy study of the peripheral olfactory organ of the guppy, *Poecilia reticulata* (Teleostei, Poecilidae). Microsc. Res. Tech. 70, 782–789. https://doi.org/10.1002/jemt.20487.

Lazzari, M., Bettini, S., Franceschini, V., 2016. Immunocytochemical characterisation of ensheathing glia in the olfactory and vomeronasal systems of *Ambystoma mexicanum* (Caudata: Ambystomatidae). Brain Struct. Funct. 221, 955–967. https://doi.org/10.1007/s00429-014-0949-8.

Lazzari, M., Bettini, S., Milani, L., Maurizii, M.G., Franceschini, V., 2017. Differential response of olfactory sensory neuron populations to copper ion exposure in zebrafish. Aquat. Toxicol. 183, 54–62. https://doi.org/10.1016/j.aquatox.2016.12.012. Lürling, M., Scheffer, M., 2007. Info-disruption:pollution and the transfer of chemical information between organisms. Trends Ecol. Evol. 22, 374–379. https://doi.org/10.1016/j.tree.2007.04.002.

Macomber, L., Elsey, S.P., Hausinger, R.P., 2011. Fructose- 1,6-bisphosphate aldolase (class II) is the primary site of nickel toxicity in *Escherichia coli*. Mol. Microbiol. 82, 1291–1300. https://doi.org/10.1111/j.1365-2958.2011.07891.x.

Michel, W.C., Sanderson, M.J., Olson, J.K., Lipschitz, D.L., 2003. Evidence of a novel transduction pathway mediating detection of polyamines by the zebrafish olfactory system. J. Exp. Biol. 206, 1697–1706.

Miyasaka, N., Wanner, A.A., Li, J., Mack-Bucher, J., Genoud, C., Yoshihara, Y., Friedrich, R.W., 2013. Functional development of the olfactory system in zebrafish. Mech. Dev. 130, 336–346. https://doi.org/10.1016/j.mod.2012.09.001.

Moran, D.T., Rowley III, J.C., Aiken, G.R., Jafek, B.W., 1992. Ultrastructural neurobiology of the olfactory mucosa of the brown trout, Salmo trutta. Microsc. Res. Technol. 23, 28–48. https://doi.org/10.1002/jemt.1070230104.

Oka, Y., Saraiva, L.R., Korsching, S.I., 2012. Crypt neurons express a single V1R-related ora gene. Chem. Senses 37, 219–227. https://doi.org/10.1093/chemse/bjr095. Poulsen, S.B., Svendsen, J.C., Aarestrup, K., Malte, H., 2014. Calcium-dependent behavioural responses to acute copper exposure in Oncorhynchus mykiss. J. Fish Biol. 84, 1326–1339. https://doi.org/10.1111/jfb.12356.

Rolen, S.H., Sorensen, P.W., Mattson, D., Caprio, J., 2003. Polyamines as olfactory stimuli in the goldfish Carassius auratus. J. Exp. Biol. 206, 1683–1696. https://doi.org/10.1242/jeb.00338.

Sandahl, J.F., Baldwin, D.H., Jenkins, J.J., Scholz, N.L., 2007. A sensory system at the interface between urban stormwater runoff and salmon survival. Environ. Sci. Technol. 41, 2998–3004.

Sato, K., Suzuki, N., 2001. Whole-cell response characteristics of ciliated and microvillous olfactory receptor neurons to amino acids, pheromone candidates and urine in rainbow trout. Chem. Senses 26, 1145–1156.

Sato, Y., Miyasaka, N., Yoshihara, Y., 2005. Mutually exclusive glomerular innervation by two distinct types of olfactory sensory neurons revealed in transgenic zebrafish. J. Neurosci. 25, 4889–4897. https://doi.org/10.1523/JNEUROSCI.0679-05.2005.

Schwarzenbach, R.P., Egli, T., Hofstetter, T.B., von Gunten, U., Wehrli, B., 2010. Global water pollution and human health. Annu. Rev. Environ. Resour. 35, 109–136. https://doi.org/10.1146/annurev-environ-100809-125342.

Scott, G.R., Sloman, K.A., 2004. The effects of environmental pollutants on complex fish behaviour: integrating behavioural and physiological indicators of toxicity. Aquat. Toxicol. 68, 369–392. https://doi.org/10.1016/j.aquatox.2004.03.016.

Scott, G.R., Sloman, K.A., Rouleau, C., Wood, C.M., 2003. Cadmium disrupts behavioural and physiological responses to alarm substance in juvenile rainbow trout (*Oncorhynchus mykiss*). J. Exp. Biol. 206, 1779–1790.

Segner, H., 2009. Zebrafish (*Danio rerio*) as a model organism for investigating endocrine disruption. Comp. Biochem. Physiol. C Toxicol. Pharmacol. 149, 187–195. https://doi.org/10.1016/j.cbpc.2008.10.099.

Simonato, J.D., Mela, M., Doria, H.B., Guiloski, I.C., Randi, M.A., Carvalho, P.S., Meletti, P.C., Silva de Assis, H.C., Bianchini, A., Martinez, C.B., 2016. Biomarkers of waterborne copper exposure in the neotropical fish Prochilodus lineatus. Aquat. Toxicol 170, 31–41. https://doi.org/10.1016/j.aquatox.2015.11.012.

Soller, J., Stephenson, J., Olivieri, K., Downing, J., Olivieri, A.W., 2005. Evaluation of seasonal scale first flush pollutant loading and implications for urban runoff management. J. Environ. Manage. 76, 309–318. https://doi.org/10.1016/j.jenvman.2004.12.007.

Song, L., Vijver, M.G., Peijnenburg, W.J., Galloway, T.S., Tyler, C.R., 2015. A comparative analysis on the in vivo toxicity of copper nanoparticles in three species of freshwater fish. Chemosphere 139, 181–189. https://doi.org/10.1016/j.chemosphere.2015.06.021.

Sorensen, P.W., Caprio, J., 1998. Chemoreception. In: Evans, D.H. (Ed.), The physiology of fishes. CRC Press, Boca Raton (FL), pp. 375–405.

Sovová, T., Boyle, D., Sloman, K.A., Vanegas Pérez, C., Handy, R.D., 2014. Impaired behavioural response to alarm substance in rainbow troutexposed to copper nanoparticles. Aquat. Toxicol. 152, 195–204. https://doi.org/10.1016/j.aquatox.2014.04.003.

Svecevičius, G., 2012. Avoidance of copper and zinc by rainbow trout *Oncorhynchus mykiss* pre-exposed to copper. Bull. Environ. Contam. Toxicol. 88, 1–5. https://doi.org/10.1007/s00128-011-0426-5.

Tierney, K.B., 2016. Chemical avoidance responses of fishes. Aquat. Toxicol. 174, 228–241. https://doi.org/10.1016/j.aquatox.2016.02.021.

Tierney, K.B., Baldwin, D.H., Hara, T.J., Ross, P.S., Scholz, N.L., Kennedy, C.J., 2010. Olfactory toxicity in fishes. Aquat. Toxicol. 96, 2–26. https://doi.org/10.1016/j.aquatox.2009.09.019.

Tiller, K.G., 1989. Heavy metals in soils and their environmental significance. Adv. Soil Sci. 9, 113–142.

Tilton, F., Tilton, S.C., Bammler, T.K., Beyer, R., Farin, F., Stapleton, P.L., Gallagher, E.P., 2008. Transcriptional biomarkers and mechanisms of copper-induced olfactory injury in zebrafish. Environ. Sci. Technol. 42, 9404–9411.

Tilton, F.A., Bammler, T.K., Gallagher, E.P., 2011. Swimming impairment and acetylcholinesterase inhibition in zebrafish exposed to copper or chlorpyrifos separately, or as mixtures. Comp. Biochem. Physiol. C Toxicol. Pharmacol. 153, 9–16. https://doi.org/10.1016/j.cbpc.2010.07.008.

Topal, A., Atamanalp, M., Oruç, E., Halıcı, M.B., Şişecioğlu, M., Erol, H.S., Gergit, A., Yılmaz, B., 2015. Neurotoxic effects of nickel chloride in the rainbow trout brain: Assessment of c-Fos activity, antioxidant responses, acetylcholinesterase activity, and histopathological changes. Fish Fisyol. Biochem. 41, 625–634. https://doi.org/10.1007/s10695-015-0033-1.

Vielma, A., Ardiles, A., Delgado, L., Schmachtenberg, O., 2008. The elusive crypt olfactory receptor neuron: evidence for its stimulation by amino acids and cAMP pathway agonists. J Exp. Biol. 211, 2417–2422. https://doi.org/10.1242/jeb.018796.

Wang, H., Liang, Y., Li, S., Chang, J., 2013a. Acute toxicity, respiratory reaction, and sensitivity of three cyprinid fish species caused by exposure to four heavy metals. PLoS One 8https://doi.org/10.1371/journal.pone.0065282. e65282.

Wang, L., Bammler, T.K., Beyer, R.P., Gallagher, E.P., 2013b. Copper-induced deregulation of microRNA expression in the zebrafish olfactory system. Environ. Sci. Technol. 47, 7466–7474. https://doi.org/10.1021/es400615q.

White, T., Hedges, K., Firth, I., 2016. Nickel and its compounds – Potential for occupational health issues. Available from:. AIOH Position paper (Cited 13 February 2018). https://www.aioh.org.au/documents/item/101.

Wu, H.H., Ivkovie, S., Murray, R.C., Jaramillo, S., Lyons, K.M., Johnson, J.E., Calof, A.E., 2003. Autoregulation of neurogenesis by GDF11. Neuron 37, 197–207. https://doi.org/10.1016/S0896-6273(02)01172-8.

Zielinski, B.S., Hara, T.J., 2006. Olfaction. In: In: Zielinski, B.S., Hara, T.J., Farrell, A.P., Brauner, C.J. (Eds.), Fish Physiology: Sensory Systems Neuroscience, vol. 25. Elsevier, San Diego, pp. 1–43. https://doi.org/10.1016/S1546-5098(06)25001-5.